A Study on the Service Load State Behavior of Reinforced Concrete Plate Member

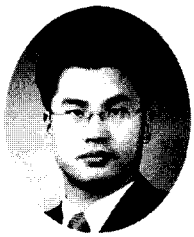

Bhang, Jee-Hwan* Kang, Won-Ho **

Abstract

This paper proposes a mechanical model to describe the load-deformation responses of the reinforced concrete plate members under service load state. An Analytical method is introduced on the basis of the rotating crack model which considers equilibrium, compatibility conditions, load-strain relationship of cracked member, and constitutive law for materials. The tension stiffening effect in reinforced concrete structures is taken into account by the average tensile stress-strain relationship from the load-strain relationship for the cracked member and the constitutive law for material. The strain compatibility is used to find out the crack direction because the crack direction is an unknown variable in the equilibrium and compatibility conditions. The proposed theory is verified by the numerous experimental data such as the crack direction, moment–steel strain relationship, moment-crack width relationship. The present paper can provide some basis for the provision of the definition of serviceability for plate structures of which reinforcements are deviated from the principal stresses, because the present code defines the serviceability by the deflection, crack control, vibration and fatigue basically for the skeletal members. The proposed theory is applicable to predict the service load state behavior of a variety of reinforced concrete plate structures such as skew slab bridges, the deck of skew girder bridges.

Keywords : service load state behavior, rotating crack model, reinforced concrete plate member, load-deformation response, crack direction, average strain, crack width

* KCI Member, Assigned Researcher, Ph.D. Dong Ah Construction Industrial Co.LTD, Koera.
** KCI Member, Professor, Ph.D. Dept of Civil and Ocean Engineering Dong-A University, Korea.

1. Introduction

It is well known that the reinforcements in reinforced concrete and plate member such as slabs are more efficient when the reinforcing bars are arranged parallel to the directions of the principal tensile stress. In this case, the bars pass through the cracks orthogonally and they can carry the tensile stresses of concrete. Therefore, the reinforcement performs best if the reinforcing bars are distributed along the trajectory of the principal stress or the principal moment. But we can find out the areas in which this ideal arrangement of reinforcement cannot be realized from the practical reason in almost all reinforced concrete plate members. Thus, a problem arises in determining the response of reinforced concrete structures consisted of plate members in which the direction of reinforcing bars are inclined to the direction of principal tensile stresses.

Typical reinforced concrete plate elements such as the skew slab bridge, the deck of skew girder bridge and the upper and lower flange of box girder are such a case. In these cases the principal stress direction does not coincide with the reinforcement direction in the reinforced concrete structures consisted of plate members although the longitudinal reinforcement direction is generally normal to the crack direction in a skeletal member. The present code defines serviceability by the deflection, crack control, vibration and fatigue of the skeletal member, but it doesn't provide any definition for plate structures of which reinforcements are deviated from the principal stresses.

When the reinforcement direction does not coincide with the principal stress direction, it is necessary to consider the reinforcement direction in a concrete plate structures for an efficient and economical analysis.

Baumann [1,2] treated the reinforced concrete plate member as if consisted of upper and lower plane stress element carrying in-plane forces, i.e. the principal moments are represented by internal force couples. But this calculation method is not suitable for the behavior of plate member under service loads. Zararis[16] presented a theory considering the stresses in reinforced concrete shear walls and plates with orthogonal reinforcements under service loads.

He proved the existence of shear forces theoretically and determines their magnitude by the compatibility condition of the strains at the cracked section. However, he did not consider the tension- stiffening effect and the concept of average stress and average strain proposed in the references.[8,14] That is to say, he did not apply his theory to the load-deformation response throughout the loading history.

However, in the proposed model the tension zone is modeled as the rotating crack model and the compressive stress distribution in the compression zone is considered to represent the behavior of reinforced concrete plate member. The expressions derived from the plane stress member are extended to those representing the behavior of the plate member after crack development. The proposed load-deformation responses are compared with the experimental results from literatures.

The research objective of this study is to present an analytical model based on the rotating crack model.[4,8,14] Since the proposed model is based on the rotating crack model, it can be easily dealt with the cases in which the reinforcements are deviated from the principal stresses. As the model uses the concept of average stress and average strain to calculate the load-deformation responses of a reinforced concrete plate member, it can be applied to calculate the service state behavior.

2. Governing Equations

A diagram of a reinforced concrete plate element subjected to normal stresses is shown in Fig. 1 (a). The directions of the longitudinal and transverse steel bars are designated as the x- and y-axes, respectively, constituting the x, y-coordinate system. Accordingly, the normal stresses are σ_x, and σ_y, and the shear stress is τ_{xy}.

When the principal tensile stress (σ_1) reaches the tensile strength of concrete, diagonal cracks will form and the concrete will be separated into a series of concrete struts by the diagonal cracks. If the element is reinforced with different amounts of steel in the x and y directions, as shown in Fig. 1 (c), the direction of the principal stresses in concrete after cracking will deviate from the direction of the applied principal stresses in Fig. 1 (b).

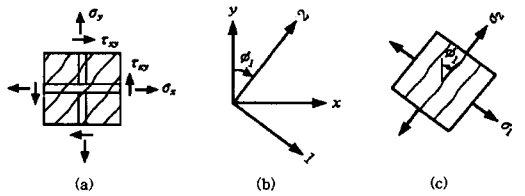

Fig.1 Definitions of stresses and coordinate system

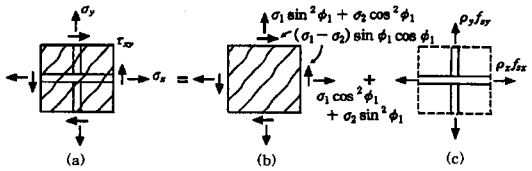

Fig. 2 Stress condition in reinforced concrete element (a) Reinforced concrete, (b) Concrete struts, (c) Reinforcement

The following assumptions will be made to describe the equilibrium conditions and compatibility conditions.

1. Stresses and strains can be expressed in terms of average values when considered areas or distances are large enough to include several cracks.
2. The concrete and the reinforcing bars are perfectly bonded together.
3. The longitudinal and transverse reinforcing bars are uniformly distributed.

2.1 Equilibrium Conditions

The stresses in the reinforced concrete element are resisted both by the concrete and the steel reinforcements. The concrete stresses in the two coordinate system x-y and 1-2 are transformed according to the usual stress transformation equations. The stresses in reinforcements are assumed to take only axial stresses.

The total stress in a reinforced concrete element is the superposition of the concrete stress and the reinforcement contributions.

$$\sigma_x = \sigma_1 \cos^2 \phi_1 + \sigma_2 \sin^2 \phi_1 + \rho_x f_{sx} \quad (1)$$

$$\sigma_y = \sigma_1 \sin^2 \phi_1 + \sigma_2 \cos^2 \phi_1 + \rho_y f_{sy} \quad (2)$$

$$\tau_{xy} = (\sigma_2 - \sigma_1) \sin \phi_1 \cos \phi_1 \quad (3)$$

σ_x, σ_y = normal stresses in the x and y directions, respectively (positive for tension)

σ_1, σ_2 = principal stresses in the 1 and 2 directions, respectively (positive for tension)

ϕ_1 = angle of inclination of the 2 direction with respect to y direction

ρ_x, ρ_y = reinforcement ratio in x and y directions, respectively

f_{sx}, f_{sy} = steel stress in x and y directions, respectively

2.2 Compatibility Conditions

The two-dimensional compatibility condition expresses the relationship among the average strains in different coordinate systems.

The transformation of average strains between the x, y coordinate system ($\varepsilon_x, \varepsilon_y, \gamma_{xy}$) and the 1, 2 principal axes ($\varepsilon_1, \varepsilon_2$) gives

$$\varepsilon_x = \varepsilon_1 \cos^2 \phi_1 + \varepsilon_2 \sin^2 \phi_1 \quad (4)$$

$$\varepsilon_y = \varepsilon_1 \sin^2 \phi_1 + \varepsilon_2 \cos^2 \phi_1 \quad (5)$$

$$\gamma_{xy} = 2(\varepsilon_1 - \varepsilon_2) \sin \phi_1 \cos \phi_1 \quad (6)$$

$$\varepsilon_x + \varepsilon_y = \varepsilon_1 + \varepsilon_2 \quad (7)$$

$\varepsilon_x, \varepsilon_y$ = average strains in the x and y directions, respectively (positive for tension)

γ_{xy} = average shear strains in x-y coordinate

$\varepsilon_1, \varepsilon_2$ = average principal strains in the 1and 2 directions, respectively (positive for tension)

3. The Mechanism of Cracking and Deformation of Plate Element

The principles of load-deformation behavior can be most easily understood by considering the mechanism of cracking of a reinforced concrete member subjected to pure bending.[6,11]

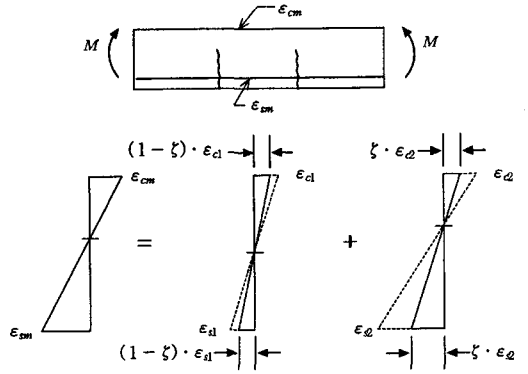

Fig. 3 Average strain of the member subjected to pure bending

As shown in Fig. 3, average strain in the concrete at the extreme compressive fiber and the average tensile strain in the reinforcing steel are given as follows.

$$\varepsilon_{cm} = (1-\zeta)\cdot\varepsilon_{c1} + \zeta\cdot\varepsilon_{c2}$$
$$\varepsilon_{sm} = (1-\zeta)\cdot\varepsilon_{s1} + \zeta\cdot\varepsilon_{s2} \quad (8)$$

ε_{c1} = concrete strain in state I

ε_{c2} = concrete strain in state II

ε_{s1} = steel strain in state I

ε_{s2} = steel strain in state II

The coefficient ζ for the member subjected to pure bending is given by Eq. (9).

$$\zeta = 1 - \beta_1 \cdot \beta_2 \cdot \left(\frac{M_{cr}}{M}\right)^2 \quad \text{for } M \geq M_{cr} \quad (9)$$

$$= 0 \quad \text{for } M < M_{cr}$$

M = maximum moment in the member at the loading stage

$$M_{cr} = \frac{I_g \cdot f_r}{y_t} = \text{the cracking moment}$$

I_g = moment of inertia in state I including the reinforcement

f_r = modulus of rupture $= 0.63 \cdot \sqrt{f_c}$ [Mpa]

y_t = the distance of the extreme tension fiber from the center of gravity of the section

β_1 = the coefficient which takes into account the bond properties
= 1.0 for high bond bars
= 0.5 for plain bars

β_2 = the coefficient which considers the deterioration of tension stiffening for long term and repeated loading
= 1.0 at first loading and
= 0.5 for long term or repeated loads independently on their duration

Evaluation of the response of a flexural member is somewhat difficult, because the stresses and strains vary over the depth of the member.

The internal lever arm for arbitrary load path is defined as follows.

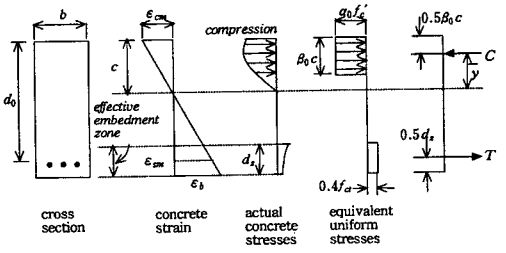

Fig. 4 Stress block factor

$$z = d_0 - \left[0.5\beta_0 - \frac{\varepsilon_{cm}}{\varepsilon_{cm} + \varepsilon_{sm}} \cdot d_0 \right] \qquad (10)$$

where

d_0= effective depth

ε_{cm} = the average strain at the extreme compressive fiber

ε_{sm} = the average strain in the reinforcement

$$\beta_0 = \frac{4 - \varepsilon_{cm} / \varepsilon_c^{'}}{6 - 2\varepsilon_{cm} / \varepsilon_c^{'}}$$

=stress-block factor for a more general concrete stress-strain relationship of a parabolic stress-strain curve

$\varepsilon_c^{'}$ = strain when concrete reaches its compressive strength($f_c^{'}$)

4. Material Law

4.1 Constitutive Laws for Concrete

The stress and strain relationship of concrete in the 2-direction is proposed by many researchers. In this model we use the material law proposed by Roos,[13] since he critically reviewed almost all the previous theories and test results. Concrete strength is based on the following equation

$$f_c^{cr} = \frac{1}{\sqrt{1 + k_{1\varepsilon} \cdot \left(1 + \frac{\Theta - \phi}{k_{2\varepsilon}} \right) \cdot \varepsilon_1}} \cdot f_c^{'} \qquad (11)$$

The factor $k_{1\varepsilon}$=160 and $k_{2\varepsilon}$=11 is determined from the experimental results.

The average principal tensile strain (ε_1) is given as a principal parameter, and the difference $\Delta\phi = (\Theta - \phi)$ of crack direction from compressive stress direction is introduced as another parameter (Fig. 5).

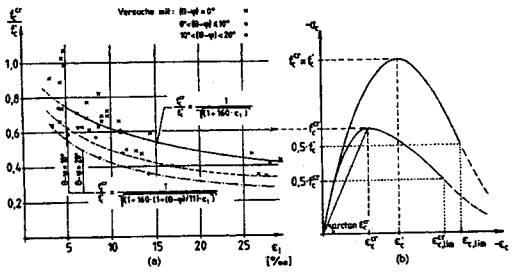

Fig. 5 Stress-strain relationships of cracked concrete

Not only the concrete compressive strength but also the compressive strain are modified by the crack development.[3,12,15] This compressive strain is proportionally applied to the compressive strength

$$\varepsilon_c^{cr} = \frac{f_c^{cr}}{f_c^{'}} \cdot \varepsilon_c^{'} \qquad (12)$$

In case that the plate is under biaxial moment as illustrated in Fig. 6, the compressive strength may be reduced due to the tensile strain (ε_1) on the same surface under the biaxial moment.

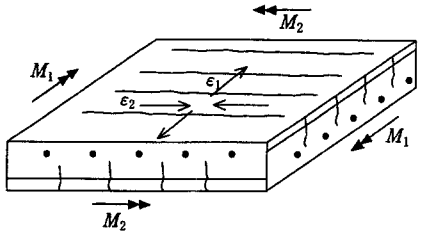

Fig. 6 Biaxial strain state of a plate element under biaxial moment

4.2 Constitutive Laws for Reinforcing Steel

The stress-strain relationships for the longitudinal and transverse mild steel can be expressed in a general manner as follows

$$f_s = f(\varepsilon_s) \tag{13}$$

where f is a function to be assumed for mild steel.

If the stress-strain relationships for longitudinal and transverse mild steel are assumed to be elastic-perfectly plastic, then

$$f_s = E_s \cdot \varepsilon_s \quad \text{when} \quad \varepsilon_s < \varepsilon_{sy}$$
$$f_s = f_y \quad \text{when} \quad \varepsilon_s \geq \varepsilon_{sy}$$

where E_s = modulus of elasticity
f_y = steel yield stress
ε_{sy} = steel yield strain

5. The Behavior of Reinforced Concrete Plate Member with Orthogonal Reinforcement

5.1 Average strains in the Reinforced Concrete Plate Element after Cracking

As a plate member is loaded under incremental moment, the lever arm, which is the distance between the resultant compressive force and the resultant tensile force, changes according to the variation of the depth of compression zone at each loading stage. The average tensile stress and strain of the reinforcement can be estimated with the effective concrete area ($A_{c,ef}$) that is computed by considering both of the reinforcement and the concrete in tension zone (Fig. 7).

The angle of the crack under service load is denoted by ϕ_1. The moments which acts on a unit element of the plate viewed in the direction of the cracks are shown in Fig. 8.

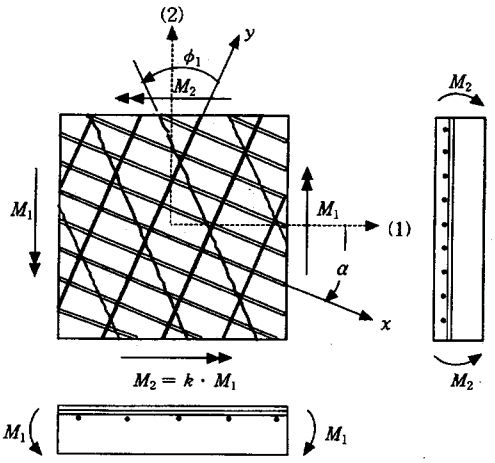

Fig. 7 The behavior of plate element by moment M_1,M_2: crack formation in the tension by bending

The moment acting at the cracked section in the x and y direction are

$$M_x = \sigma_x \cdot A_{sx} \cdot z_x \tag{14}$$

$$M_y = \sigma_y \cdot A_{sy} \cdot z_y \tag{15}$$

The lever arm z_x, z_y are defined as shown in Eq.(10)

If the crack direction (ϕ_1) is known, the moment equilibrium on the section parallel to the crack direction can be represented according to Fig. 8. The equilibrium equation can be obtained at the cracked section as follows.

$$M_x b_x \cos\phi_1 + M_y b_y \sin\phi_1 \quad (16)$$
$$= M_1 b_1 \cos(\phi_1 - \alpha) + M_2 b_2 \sin(\phi_1 - \alpha)$$

$$-M_x b_x \sin\phi_1 + M_y b_y \cos\phi_1 \quad (17)$$
$$= -M_1 b_1 \sin(\phi_1 - \alpha) + M_2 b_2 \cos(\phi_1 - \alpha)$$

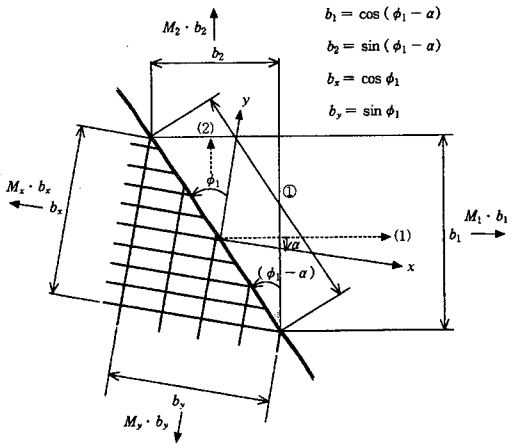

Fig. 8 The equilibrium between the external moment and the internal resistance in a plate element carrying moment at a cracked section

The width b_1 to b_y, on which the moments M_1 to M_y act, are represented as a function of α and ϕ_1. The moments at the cracked section in the x and y direction are

$$M_x = \cos^2\alpha(1+\tan\alpha\tan\Phi_1)M_1 + \sin^2\alpha(1-\cot\alpha\tan\Phi_1)M_2 \quad (18)$$

$$M_y = \sin^2\alpha(1+\cot\alpha\cot\Phi_1)M_1 + \cos^2\alpha(1-\tan\alpha\cot\Phi_1)M_2 \quad (19)$$

M_{xy} can be represented in the case that M_1 is a different sign convention from M_2.

The average steel forces in the reinforcement after crack development are Eqs. (20) and (21).

If the unit length normal to the crack direction is considered as shown in Fig. 9, the force equilibrium including the diagonal compressive force D_c can be obtained.

The diagonal compressive force D_c in Eq.(22) is represented from the $N_{sr,x}$, $N_{sr,y}$, M_1/z_m and M_2/z_m.

After the introduction of $N_{sr,x}$ and $N_{sr,y}$ from Eq.(20), (21) and the given width b_1 to b_y in Fig. 9, the following relationship can be obtained as in Eq. (23).

$$N_{sr,x} = M_x / z_x - \frac{\beta_1\beta_2\sigma_{sr,x}^2 A_{sx}^2}{M_x / z_x}$$
$$= \left[\cos^2\alpha(1+\tan\alpha\tan\Phi_1)\frac{M_1}{z_x} + \sin^2\alpha(1-\cot\alpha\tan\Phi_1)\frac{M_2}{z_x}\right]$$
$$-\left[\frac{\beta_1\beta_2\sigma_{sr,x}^2 A_{sx}^2}{\cos^2\alpha(1+\tan\alpha\tan\Phi_1)\frac{M_1}{z_x} + \sin^2\alpha(1-\cot\alpha\tan\Phi_1)\frac{M_2}{z_x}}\right] \quad (20)$$

$$N_{sr,y} = M_y / z_y - \frac{\beta_1\beta_2\sigma_{sr,y}^2 A_{sy}^2}{M_y / z_y}$$
$$= \left[\sin^2\alpha(1+\cot\alpha\cot\Phi_1)\frac{M_1}{z_y} + \cos^2\alpha(1-\cot\alpha\tan\Phi_1)\frac{M_2}{z_y}\right]$$
$$-\left[\frac{\beta_1\beta_2\sigma_{sr,y}^2 A_{sy}^2}{\sin^2\alpha(1+\cot\alpha\cot\Phi_1)\frac{M_1}{z_y} + \cos^2\alpha(1-\tan\alpha\cot\Phi_1)\frac{M_2}{z_y}}\right] \quad (21)$$

$N_{sr,x}$: steel force in x-direction after cracking
$N_{sr,y}$: steel force in y-direction after cracking

The mean lever arm (z_m) for the principal moments is taken approximately as $z_m \approx (z_x + z_y)/2$ at each loading step.

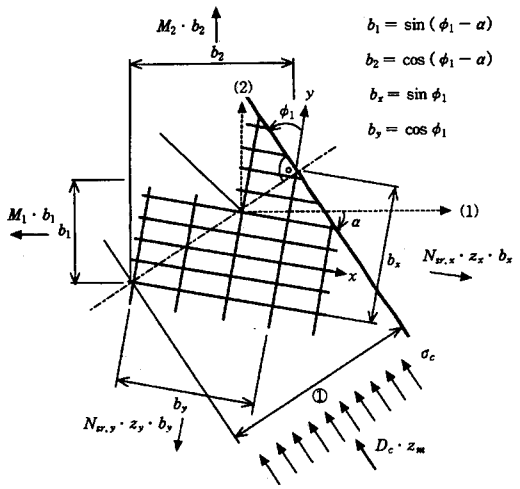

Fig. 9 The equilibrium in diagonal compressive strut over unit width between the external moment and the internal resistance in a plate element

$$D_c = N_{sr,x} b_x \sin\phi_1 + N_{sr,y} b_y \cos\phi_1 - \frac{M_1}{z_m} b_1 \sin(\phi_1 - \alpha) - \frac{M_2}{z_m} b_2 \cos(\phi_1 - \alpha)$$
$$= N_{sr,x} \sin^2\phi_1 + N_{sr,y} \cos^2\phi_1 - \frac{M_1}{z_m} \sin^2(\phi_1 - \alpha) - \frac{M_2}{z_m} \cos^2(\phi_1 - \alpha) \quad (22)$$

$$D_c = \left(\frac{M_1}{z_m} - \frac{M_2}{z_m}\right) \frac{\sin\alpha \cos\alpha}{\sin\phi_1 \cos\phi_1} - \left[\frac{\beta_1 \beta_2 \sigma_{sr,x}^2 A_{sx}^2 \sin\phi_1 \cos\phi_1}{\left(\frac{M_1}{z_x} - \frac{M_2}{z_x}\right)\sin\alpha \cos\alpha + \left(\frac{M_1}{z_x} + \frac{M_2}{z_x}\right)\cot\phi_1} + \frac{\beta_1 \beta_2 \sigma_{sr,y}^2 A_{sy}^2 \sin\phi_1 \cos\phi_1}{\left(\frac{M_1}{z_y} - \frac{M_2}{z_y}\right)\sin\alpha \cos\alpha + \left(\frac{M_1}{z_y} + \frac{M_2}{z_y}\right)\tan\phi_1} \right] \quad (23)$$

It is noted that ε_x and ε_y can be taken from the average strain concept after cracking as follows

$$\varepsilon_x = \frac{1}{A_{sx} E_s} \left[\frac{M_x}{z_x} - \frac{\beta_1 \beta_2 \sigma_{sr,x}^2 A_{sx}^2}{\frac{M_x}{z_x}} \right]$$
$$= \frac{1}{A_{sx} E_s} \left[\cos^2\alpha \left(1 + \tan\alpha \tan\phi_1\right) \frac{M_1}{z_x} + \sin^2\alpha \left(1 - \cot\alpha \tan\phi_1\right) \frac{M_2}{z_x} - \left(\frac{\beta_1 \beta_2 \sigma_{sr,x}^2 A_{sx}^2}{\cos^2\alpha \left(1 + \tan\alpha \tan\phi_1\right) \frac{M_1}{z_x}} \right. \right.$$
$$\left. \left. + \sin^2\alpha \left(1 - \cot\alpha \tan\phi_1\right) \frac{M_2}{z_x} \right) \right] \quad (24)$$

$$\varepsilon_y = \frac{1}{A_{sy} E_s} \left[\frac{M_y}{z_y} - \frac{\beta_1 \beta_2 \sigma_{sr,y}^2 A_{sy}^2}{\frac{M_y}{z_y}} \right]$$
$$= \frac{1}{A_{sy} E_s} \left[\sin^2\alpha \left(1 + \cot\alpha \cot\phi_1\right) \frac{M_1}{z_y} + \cos^2\alpha \left(1 - \tan\alpha \cot\phi_1\right) \frac{M_2}{z_y} - \left(\frac{\beta_1 \beta_2 \sigma_{sr,y}^2 A_{sy}^2}{\sin^2\alpha \left(1 + \cot\alpha \cot\phi_1\right) \frac{M_1}{z_y}} \right. \right.$$
$$\left. \left. + \cos^2\alpha \left(1 - \tan\alpha \cot\phi_1\right) \frac{M_2}{z_y} \right) \right] \quad (25)$$

Principal compressive strain (ε_2) can be obtained from the diagonal compressive force parallel to the crack direction

$$\varepsilon_2 = -\frac{D_c}{h_m \cdot E_c}$$

$$= -\frac{1}{h_m \cdot E_c}\left[\left(\frac{M_1}{z_m}-\frac{M_2}{z_m}\right)\frac{\sin\alpha\cos\alpha}{\sin\phi_1\cos\phi_1}\right.$$

$$-\left(\frac{\beta_1\beta_2\sigma_{sr,x}^2 A_{sx}^2 \sin\phi_1\cos\phi_1}{\left(\frac{M_1}{z_y}-\frac{M_2}{z_x}\right)\sin\alpha\cos\alpha+\left(\frac{M_1}{z_y}+\frac{M_2}{z_x}\right)\cot\phi_1}\right.$$

$$\left.\left.+\frac{\beta_1\beta_2\sigma_{sr,y}^2 A_{sy}^2 \sin\phi_1\cos\phi_1}{\left(\frac{M_1}{z_y}-\frac{M_2}{z_x}\right)\sin\alpha\cos\alpha+\left(\frac{M_1}{z_y}+\frac{M_2}{z_x}\right)\tan\phi_1}\right)\right] \quad (26)$$

where

$$h_m = \frac{h_{x,ef}+h_{y,ef}}{2}$$

= the mean depth of the effective area of concrete in tension

Principal tensile strain (ε_1) from the strain compatibility conditions is

$$\varepsilon_1 = \varepsilon_x + \varepsilon_y - \varepsilon_2 \quad (27)$$

5.2 The Crack Direction of a Plate Element in the Elastic Range of the Reinforcement in Both Directions

The strain compatibility condition can be used to determine the unknown crack direction(ϕ_1).

The compatibility condition and Eqs. (24), (25), (26), and (27) yield the following equation with consideration on the crack direction under service load state. The lever arms of z_x and z_y can be reasonably assumed to estimate the crack direction(ϕ_1) as the mean lever arm of $z_{cm} \approx 0.9 \cdot d_x$ in the x and y directions.

$$\varepsilon_1 \cos^2\Phi_1 + \varepsilon_2 \sin^2\Phi_1 = \varepsilon_x \quad (28)$$

After some manipulation to obtain the crack direction (ϕ_1) in the plate element, the following equation for the crack direction under the service load state can be obtained.

$$\Phi_1^4 + \Phi_1^3\frac{(\tan a + k\cot a)}{(1-k)} - \Phi_1\frac{(\cot a + k\tan a)}{\lambda(1-k)} - \frac{1}{\lambda}$$

$$+\Phi_1^2\frac{\beta_1\beta_2\sigma_{sr,x}^2 A_{sx}^2}{\lambda\sin a\cos a(1-k)(l\sin a\cos a + m\cdot\Phi_1)}\cdot\left[\frac{(1+\nu_m)+(1-\nu_m)\Phi_1^2}{1+\Phi_1^2}\right]$$

$$+\Phi_1^2\frac{\beta_1\beta_2\sigma_{sr,y}^2 A_{sy}^2}{\lambda\sin a\cos a(1-k)(l\sin a\cos a + m/\Phi_1)}\cdot\left[\frac{(\nu_m-\lambda)-(\nu_m+\lambda)\Phi_1^2}{1+\Phi_1^2}\right]$$

$$= \frac{\nu_m}{\lambda}\left(1-\Phi_1^4\right) \quad (29)$$

Φ_1 = $\cot\phi_1$, the crack angle from the transverse reinforcement direction

k = the ratio of minimum principal moment and maximum principal moment (M_2/ M_1)

$$l = \frac{M_1}{z_{cm}}\left(\frac{M_1}{z_{cm}}-\frac{M_2}{z_{cm}}\right)$$

$$m = \frac{M_1}{z_{cm}}\left(\frac{M_1}{z_{cm}}+\frac{M_2}{z_{cm}}\right)$$

λ = ratio of reinforcement contents(A_{sx}/A_{sy})

v_m = ratio of the stiffness of reinforcement (x) and the modulus of elasticity of the concrete

$$\rho_{x,m} \cdot E_s/E_c \text{ , where } \rho_{x,m} = A_{sx}/h_m \cdot 1$$

A positive real root of this equation gives the angle (ϕ_1) of the crack direction in a plate element under service load state when the reinforcement stress is below the yield strength (f_y). This crack direction is dependent on the ratio of reinforcement contents, the ratio of maximum principal moment and minimum principal moment and the reinforcement direction laid in the plate element

5.3 Crack Width Calculation in the Plate Element

As cracks propagate due to the external loading, the cracking is more likely to approach a stabilized state. In this state, the average crack width will be equal to the average spacing of the crack multiplied by the average strain in the reinforcement.[5,6]

Therefore, the crack width (w) in the plate element can be taken as the product of the principal tensile strain (ε_1) and the average spacing of the diagonal cracks ($l_{s,max}$).

$$w = \varepsilon_1 \cdot l_{s,max} \tag{30}$$

The spacing of the inclined cracks will depend upon the crack control characteristics of the longitudinal and transverse reinforcements, respectively. It is suggested in reference [7] that this spacing should be taken as

$$l_{s,\max} = \left(\frac{\cos\theta}{l_{sx,\max}} + \frac{\sin\theta}{l_{sy,\max}} \right)^{-1} \tag{31}$$

Thus, θ denotes the angle between the reinforcement in the x-direction and the direction of the principal tensile stress. $l_{sx,max}$ is the average crack spacing of a member subjected to longitudinal tension while $l_{sy,max}$ is the average cracking spacing of the member subjected to a transverse tension.

Average crack spacing has been empirically modified to give the following relationship in CEB-FIP MC78.

$$l_{sx,\max} = 2\left(c_{bx} + \frac{s_x}{10} \right) + k_1 \cdot k_2 \cdot \frac{\Phi_{sx}}{\rho_{x,ef}} \tag{32}$$

$$l_{sy,\max} = 2\left(c_{by} + \frac{s_y}{10} \right) + k_1 \cdot k_2 \cdot \frac{\Phi_{sy}}{\rho_{y,ef}} \tag{33}$$

c_b = clear concrete cover (mm)

s = maximum spacing of reinforcing bars but less than $15 \cdot \phi_s$

k_1 = 0.4 for deformed bars
0.8 for plain bars or bonded strands

k_2 = 0.125 for pure bending
0.25 for pure tension

6. Verification of Theoretical Proposal

The response of reinforced concrete plate subjected to uniaxial bending and pure torsion has been extensively investigated by Lenschow[10] and Iványi and Lardi.[9]

6.1 Lenschow's Plate Element Test

Lenschow[10] performed experiments on plates having a thickness of 4.14^{in} and a width of 42^{in} and a length of 90^{in} with orthogonal reinforcements, which concerned plates carrying uniaxial bending(M_{II}=0) or pure torsion (M_{II}= -M_I).

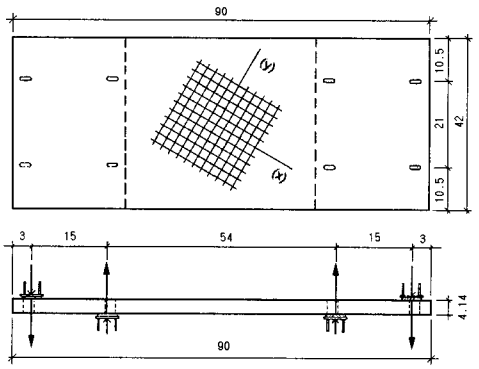

Fig. 10 The specimen under uniaxial bending tested by lenschow [unit: inch]

A list of the analyzed plates including the ratios of longitudinal and transverse reinforcements with No. 2 bars (0.25^{in} diam.), concrete strength, and reinforcement deviation angle (α) are given in Table. 1.

Table 1 Material properties for lenschow's pecimens

Plate	Concrete strength	Yield Stress	Steel direction and spacing Top/bottom			
	fc'	Fy	α1	a1/a°1	α2	a2/a°2
	[psi]	[psi]	[°]	[in.]	[°]	[in.]
B6	4890	50000	67.5°	1.5/0	-22.5°	1.375/0
B9	3820	50000	-45°	3.0/0	45°	1.375/0
B11	4800	50000	-22.5°	1.5/0	67.5°	2.75/0
B21	5180	47800	90°	1.5/1.5	0°	5.5/5.5
B22	5460	53700	90°	1.5/1.5	0°	5.5/5.5

6.1.1 Comparison of crack direction under service loads

The patterns of crack direction (ϕ_l) under service loads of the test plates with different reinforcement ratio in two orthogonal directions are shown in Fig. 11~Fig. 15 and compared with the corresponding crack directions (ϕ_l) given by the proposed expression. The crack directions (ϕ_l) indicated on the figures are calculated by the proposed expression from the beginning of cracking to the failure of plate. That is why the range of crack directions are shown.

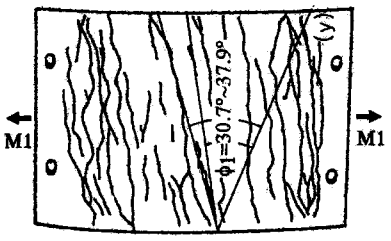

Fig. 11 Crack direction of plate B6

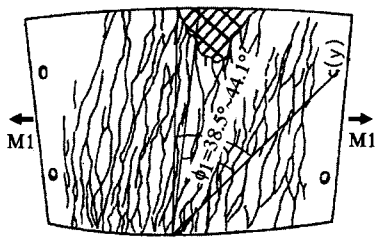

Fig. 12 Crack direction of plate B9

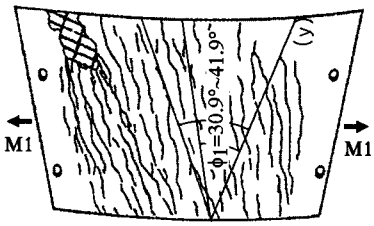

Fig. 13 Crack direction of plate B11

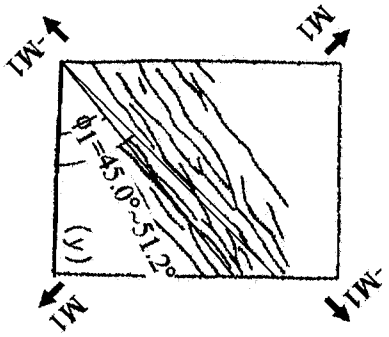

Fig. 14 Crack direction of plate B21

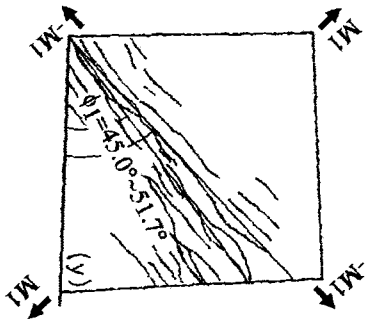

Fig. 15 Crack direction of plate B22

6.1.2 Comparison of moment-strain response of plate

Lenschow[10] obtained the steel strains of all the plates for the bending loads up to the failure.

Two reinforcing bars in each layer of reinforcement were instrumented with electric strain gages placed well within the test area. The measured strain values were plotted and shown from the measured data. It can be shown in Fig. 16~Fig.25 that the comparison between experimental and the theoretical results shows good agreements at the service loads.

The steel strains of B6, B9 and B11 are elastic under the load of 4000 lb-in/in after the cracking of tension zone that is in the tensile reinforcement as shown in Fig. 16~Fig. 21.

In the case of biaxial bending experiment of B21 and B22, the plates B22 is elastic under 3000 lb-in/in, which can be shown in Fig. 22~Fig. 25 in the case of biaxial bending.

From the figures, it can be observed that the values of strain gage placed between the crack planes are higher than the average strain value, and the values of strain gage placed in the concrete between the cracks are lower than the average strain value. This is the reason why the scatter values are shown in the measurements.

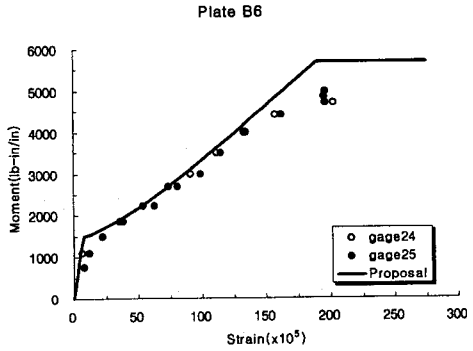

Fig. 16 Moment-strain of reinforcement in the *x* direction of plate B6

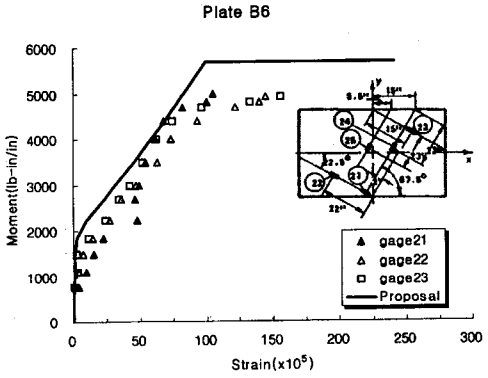

Fig. 17 Moment-strain of reinforcement in the *y* direction of plate B6

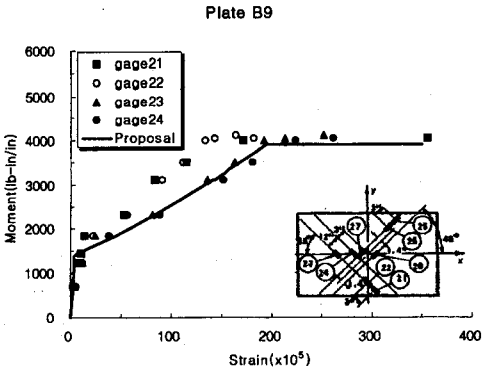

Fig. 18 Moment-strain of reinforcement in the *x* direction of plate B9

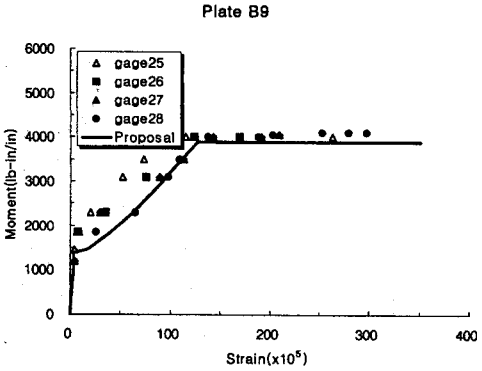

Fig. 19 Moment-strain of reinforcement in the *x* direction of plate B9

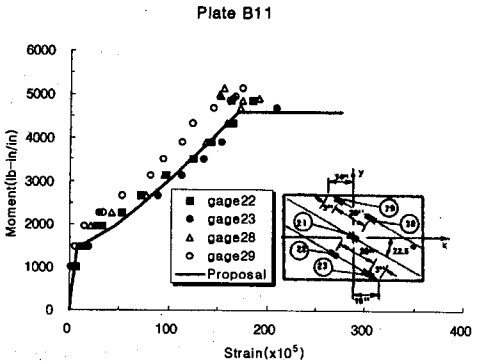

Fig. 20 Moment-strain of reinforcement in the *x* direction of plate B11

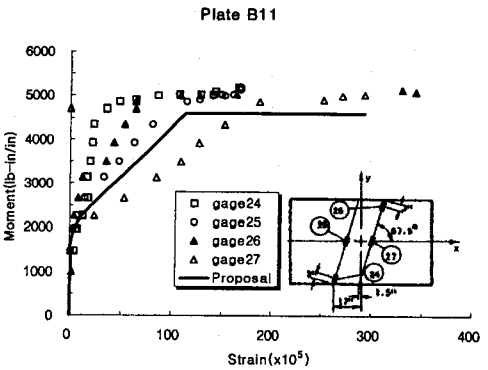

Fig. 21 Moment-strain of reinforcement in the *y* direction of plate B11

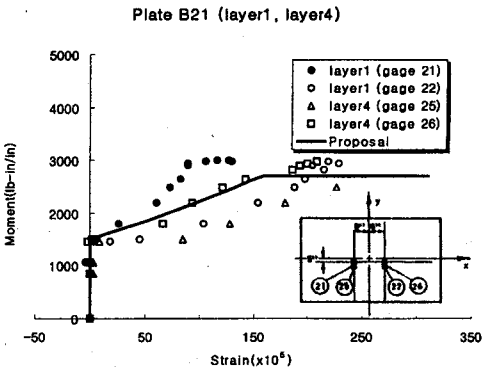

Fig. 22 Moment-strain of reinforcement in layer 1, 4 of plate B21

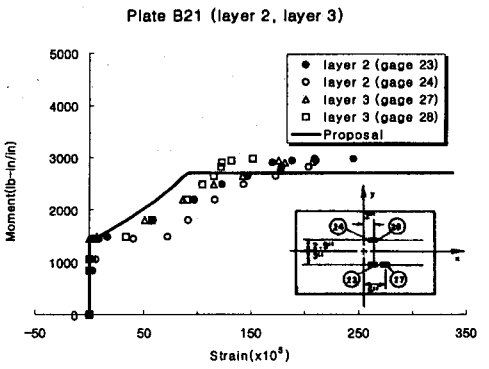

Fig. 23 Moment-strain of reinforcement in layer 2, 3 of plate B21

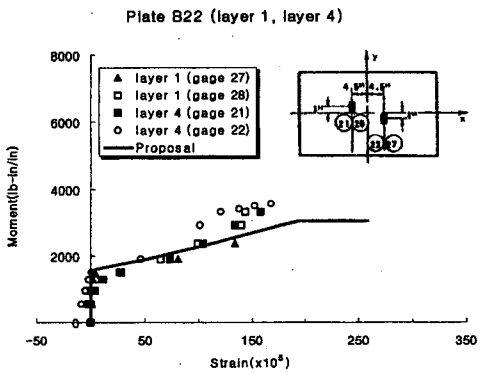

Fig. 24 Moment-strain of reinforcement in layer 1, 4 of plate B22

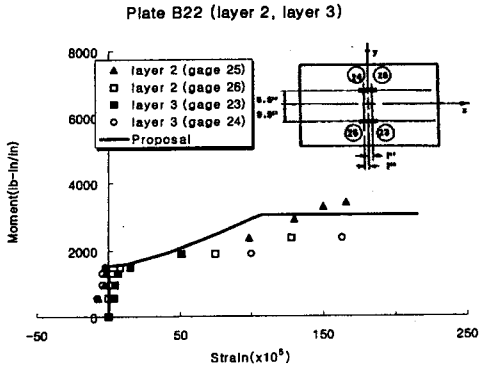

Fig. 25 Moment-strain of reinforcement in layer 2, 3 of plate B22

6.2 Iványi and Lardi's Plate Element Test

Experiments of plates subjected to uniaxial moment were performed by Iványi-Lardi[9]. The plates had a thickness of 15cm, a width of 180cm and a length of 440cm and were reinforced with orthogonal nets of reinforcing steels. The ratios of longitudinal and transverse reinforcements of the selected specimens are λ=1 in plate P8, P9, P12, P14, P15, λ=5 in plate P3, P7, P11 and λ=2 in plate P13 under uniaxial bending.

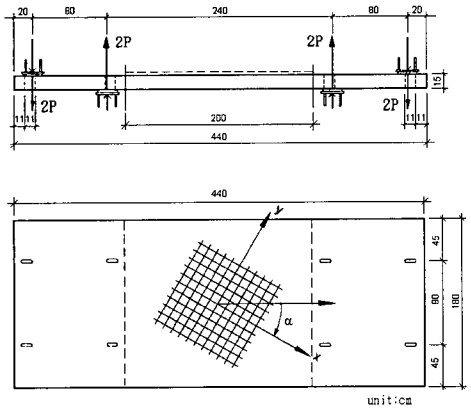

Fig. 26 The specimen under uniaxial bending tested by Iványi-Lardi [unit:cm]

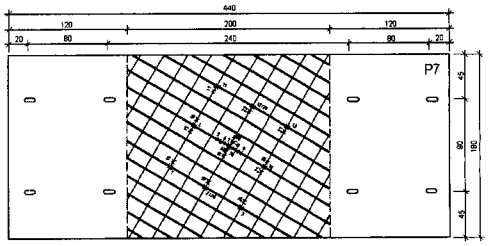

Fig. 27 Strain gage position in the reinforcement (P7)

Table. 2 Material properties of Lardi & Iványi's specimens

Plate	Concrete Strength	Reinforcement Direction and ratio			Yield Stress	
	fc'	α	ρ_x	λ	x-dir	y-dir
	[Mpa]	[°]	[%]		[Mpa]	[Mpa]
P7	24.1	30°	0.82	5	532.0	554.6
P8	22.2	30°	0.82	1	550.5	486.9
P12	31.5	30°	0.52	1	540.0	537.7
P13	27.4	30°	0.82	2	489.0	449.3
P14	25.6	30°	1.2	5	477.2	552.3

6.2.1 Comparison of crack direction under service loads

The proposed crack directions are compared with the experimental crack directions under a service load state on the test plates with different reinforcement ratios in the orthogonal directions in Table. 3.

Table 3 Comparison of crack direction

Plate	α	ρ_x	λ	Experiment	Proposal
	[°]	[%]		[°]	[°]
P8	30°	0.82	1	37.5°~42.5°	39.6°~40.1°
P12	30°	0.52	1	37.5°~37.5°	37.7°~39.0°
P13	30°	0.82	2	37.5°~42.5°	43.1°~45.0°
P7	30°	0.82	5	37.5°~42.5°	50.4°~52.8°
P14	30°	1.2	5	35.0°~40.0°	52.5°~53.0°

The patterns of crack directions in the experiment are shown in comparison with the proposed crack directions in Fig. 28 to Fig. 32. The proposed crack directions coincide well with the experimental results.

The crack direction of a plate element becomes more acute to the longitudinal reinforcement with the increase of the reinforcement ratio (λ). However, it is not influenced by the reinforcement contents (ρ_x) according to the proposal.

6.2.3 Comparison of crack width under service loads

The measurement of crack widths is carried out by means of the eye gage on the tension zone of 1.8^m x 2.0^m of the test area.

The proposed crack widths ($w_{cal,s78}$) are the product of the proposed principal tensile strain(ε_1) and the average crack spacing ($l_{s,max}$) based on the Model Code 78.

The mean crack widths (w_m) are plotted in Fig. 33 and Fig. 34 with respect to the loading history and compared with the calculated crack widths ($w_{cal,s78}$) as the product of the principal tensile strain(ε_1) and the expression of average crack spacing in section 4.3.

It may be noted that the proposed principal tensile strain (ε_1) is not estimated at the reinforcing bar, but at the plate bottom surface.

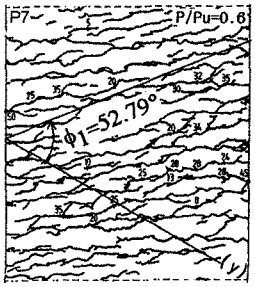

Fig. 28 Crack direction of plate P7

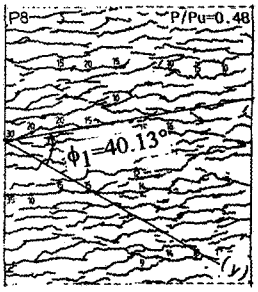

Fig. 29 Crack direction of plate P8

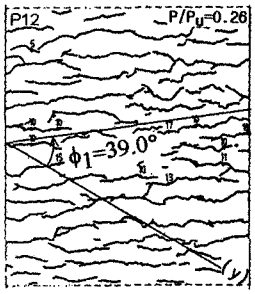

Fig. 30 Crack direction of plate P12

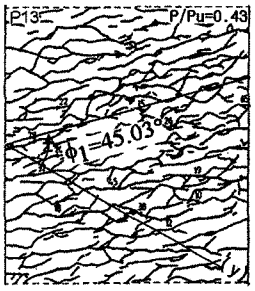

Fig. 31 Crack direction of plate P13

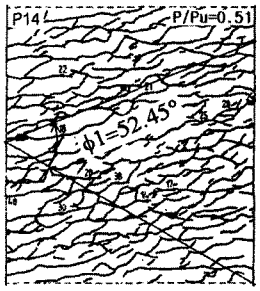

Fig. 32 Crack direction of plate P14

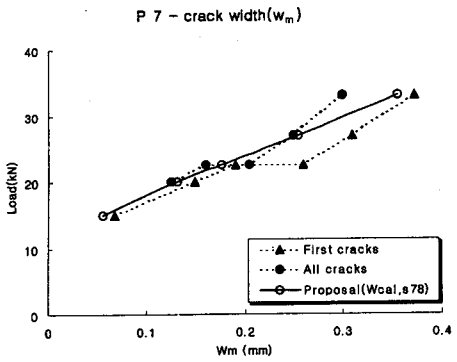

Fig. 33 Response of load-crack width for plate P7

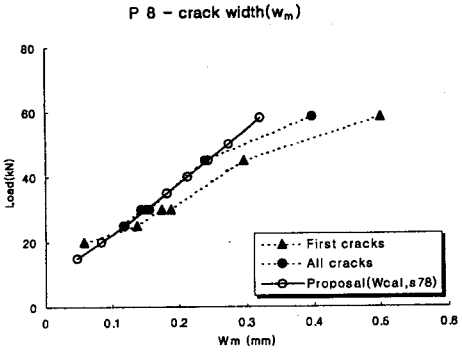

Fig. 34 Response of load-crack width for plate P8

6.2.4 Comparison of load-strain response of plate

Iványi and Lardi[9] obtained the load-deformation behavior of the plates by attaching the strain gages on the reinforcement in the tension zone. The measured steel strains ε_x and ε_y correspond to the mean values of all strain gage measurements. Plates P8, P9, P12 and P15 have the reinforcement ratio of 1.0 and the reinforcement content of 0.82, 0.82, 0.52 and 1.2 respectively, and Plate P13 has the reinforcement ratio of 2.0 and the reinforcement content of 1.2.

Although the plotted strains of test are the average values of the measurement, it is not based on the concept of average strain because the values are not from the total strain concept, but from only the strain of reinforcement. Thus it can be seen that the measured strains somewhat exceed the proposed steel strains at the same load stage. Yield plateau is determined simply from the equilibrium condition when one of the reinforcement in x and y directions reaches the yield stress(f_y).

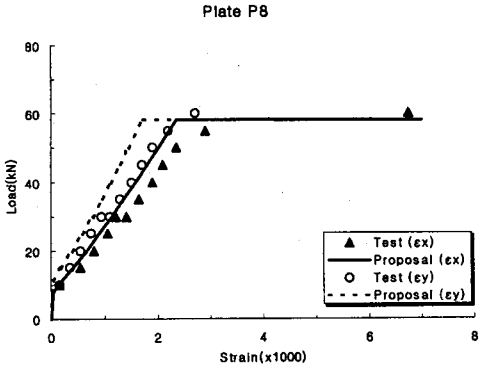

Fig. 35 Load-strain response of plate P8

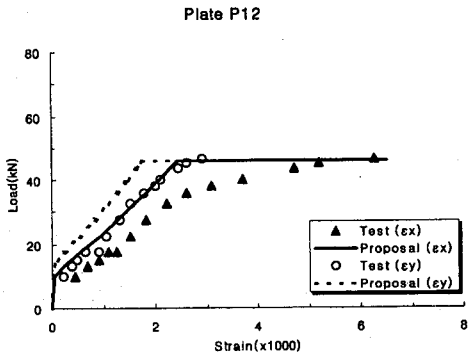

Fig. 36 Load-strain response of plate P12

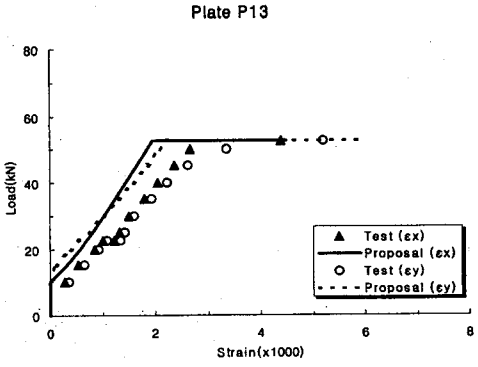

Fig. 37 Load-strain response of plate P13

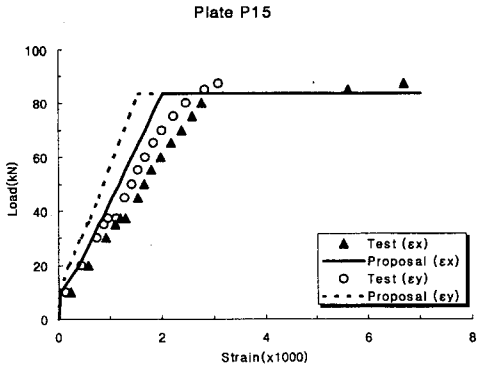

Fig. 38 Load-strain response of plate P15

7 . Conclusion

A mechanical model is proposed to describe the behavior of the plate member, which is based on the rotating crack model considering equilibrium, compatibility conditions, loaddeformation response of cracked member, and constitutive law for material. Numerous experimental data are compared with theoretical results to verify the proposed model.

1. The unknown crack directions can be directly determined by the proposed theory based on the equilibrium and the compatibility conditions, which show good agreements with the experimental results under service load state .
2. It can be observed that the crack direction of the plate becomes wider from the transverse reinforcement with the increase of the reinforcement ratio (λ) in the plate element. It is confirmed that the direction of principal tensile stress changes with the monotonically increasing loading.
3. The load-deformation responses such as moment-strain relationship, moment-crack width relationship by the proposed theory show good agreements with test results before ultimate state of the plate element. The theoretical crack width calculated by the multiplication of the average tensile strain (ε_1) of the proposed expression and the crack spacing can be applied to predict the crack width of the slab type structures.
4. The tension stiffening effect in reinforced concrete structures can be taken into account by introducing the average tensile stress-strain relationship of cracked concrete members.
5. The proposed theory is applicable to predict the service load state behavior of a variety of concrete structures such as slab bridges, deck of girder bridges.

References

1. Baumann, TH., "Tragwirkung orthogonaler bewehrungsnetze beliebiger richtung in Netzbewehrung von Flächentragwerken aus stahlbeton," DAfStb., Heft. 217, Berlin, Verlag W. Ernst&Sohn, 1972.
2. Baumann, TH., "Zur Frage der Netzbewehrung von Flächentragwerken," Bauingenieur 47, Heft.10, 1972, s.367-377.
3. Belarbi, A., Hsu, T. T. C., "Constitutive Laws of Reinforced Concrete in Biaxial Tension-Compression," Research Report UHCEE 91-2, University of Houston, 1991.
4. Bhang, J. H., Kang, W. H., "The Service State Behavior of Reinforced Concrete Membrane Elements using Rotating Crack Model," KCI, Concrete Journal, Vol. 11, No.3, 1999.
5. CEB-FIP, "Model Code for Concrete Structures(1978)", CEB-FIP International Recommendations, 3rd ed., Comité Euro-International du Béton, 1978, Paris, pp. 348.
6. CEB, "CEB Design Manual on Cracking and deformations," CEB, 1985.
7. CEB-FIP, "Model Code for Concrete Structures(1990)," CEB-FIP International Recommendations, 3rd ed., Comité Euro-International du Béton, Paris, 1991, pp. 437.
8. Hsu, Thomas T. C., "Nonlinear Analysis of Concrete Membrane Elements," ACI Structural Journal, V.88, No.5, Sep.-Oct., 1991, pp.624-635.
9. Iványi, Lardi, "Trag und Verformungsverhalten

von netzbewehrten Stahlbetonplatten," Heft 19, Forschungsberichte aus dem Fachbereich Bauwesen, Universität Essen Gesamthochschule, August, 1982.
10. Lenschow, "A Yield Criterion for Reinforced Concrete under Biaxial Moments and Forces," Dissertation, University of Illinois, 1966.
11. Manfred Wicke, "CEB-FIP Model Code 1990 Serviceability Limit States," CEB.
12. Pang, X, B., "Constitutive Law of Reinforced Concrete in Shear," Dissertation, University of Houston, 1991.
13. Roos, Winfried, "Zur Druckfestigkeit des gerissenen Stahlbetons in scheibenförmigen Bauteilen bei gleichzeitig wirkender Querzugbelastung," Dissertation,Technical Universität München, 1995, pp.174.
14. Vecchio, F., and Collins, M. P., "Modified Compression-Field Theory for Reinforced Concrete Elements subjected to Shear," ACI, Structural Journal, V.83, No.2, 1986, pp.219-231.
15. Vecchio, Frank J. and Collins, Michael P., "The Response of Reinforced Concrete To In-Plane Shear and Normal Stresses," publication No. 82-03, Department of Civil Engineering, University of Toronto, Mar, 1982, pp.332.
16. Zararis, P. D., "State of Stress in RC Plates under Service Conditions," ASCE, Journal of Structural Engineering, Vol.112, No.8, 1986, pp.1908-1927.